MADRID
inter.noise 2019
June 16 - 19
NOISE CONTROL FOR A BETTER ENVIRONMENT

Application of impact hammers without inbuilt force transducer towards isolator dynamic stiffness and blocked force measurements

Patil, Nikhilesh[1]
Acoustics Research Centre
University of Salford, Manchester, M5 4WT, UK

ABSTRACT

In-situ characterisation of structure borne sources and resilient elements (e.g. isolators/elastomeric mounts, springs) are important steps in diagnosis of noise and vibration issues. Such characterisation techniques involve measurement of Frequency Response Functions (FRF's) using an impact hammer or shaker excitation. While both excitation techniques are well developed, the impact hammer is widely in use for its ease of application. The impact hammer comes with an inbuilt force sensor to measure the contact force during excitation. The current paper presents an alternative way of using a standard tool hammer (without any inbuilt force sensor) to measure the same FRF's. The method employs measurement of transmissibility functions which only requires accelerometers. A case study is presented where the blocked forces of the source and the dynamic transfer stiffness of isolators is measured in-situ using the alternative hammer technique. The results are then compared to results obtained from a standard impact hammer (with force sensing). The new hammer technique provides excellent agreement in FRF measurement and source and isolator characterisation. The technique validates as a potential alternative for impact testing especially when standard impact testing tools are not available.

Keywords: Frequency Response Functions, Blocked forces, Dynamic transfer stiffness
I-INCE Classification of Subject Number: 41, 46, 71, 72

1. INTRODUCTION

A number of structural analysis techniques such as modal testing, source characterisation, Transfer Path Analysis (TPA), experimental substructuring, etc. are widely used in a variety of noise and vibration design and diagnosis applications. An important step in these procedures is the measurement of passive properties of the structure namely Frequency Response Functions (FRF's). FRF's are typically measured by exciting the structure at the excitation Degree(s) of Freedom (DOF) and simultaneously measuring the excitation and resultant response at the DOF of interest. Depending on the type of application and test structure, different excitation options can be employed such as impact hammer, electrical shaker, electromagnetic shaker, etc [1].

[1] n.patil1@salford.ac.uk

Of these, the impact hammer owing to its easy setup and use, is widely used. FRF's that can be measured by impact testing are highlighted in Table 1.

Table 1 FRF's that can be measured using impact testing

Accelerance	acceleration/force (a/f)
Mobility	velocity/force (v/f)
Receptance	displacement/force (x/f)
Vibroacoustic FRF	sound pressure/force (p/f)
Rotational FRFs [2]	angular velocity/moment (α/Γ)
Acoustic FRF's [3]	sound pressure/volume velocity (p/Q)

2. HAMMERS WITHOUT INBUILT FORCE SENSORS

Impact hammers come with an inbuilt force sensor to measure the contact force on impact. This contact force is then used to calculate the FRF along with the response signal. Therefore, the inbuilt force sensor is vital for the impact test. If a hammer without an inbuilt force sensor is used, then excitation of the system is still possible. However, in this case, FRF's (referenced to force) cannot be measured directly as there is no force sensor but other properties such as displacement transmissibility functions could still be measured [4]. It is therefore of interest to investigate if force referenced FRF's could be measured indirectly without the use of a force sensor.

2.1 Contact force measurement

Let us consider a tool hammer without any inbuilt force sensor to be used in impact testing. Provided the dynamic behaviour of the hammer is linear, one possible way to measure the contact force exerted by the hammer on impact is equal to the mass of the hammer times the acceleration of the hammer head upon impact. To put this into practice, the hammer must be instrumented with an accelerometer on its head. In [5], the application of a sledge hammer towards FRF measurement utilising this concept was first discussed. Results were limited to low frequency and errors were present at frequencies of internal resonances of the hammer. This is because the static mass term does not account for the dynamic characteristics (for e.g. internal resonances) of the hammer. If a hammer without force transducer is to be used, then it is desirable to derive the force from acceleration in a way that accounts for the dynamic characteristics of the hammer body. In other words, the hammer should be characterised.

2.2 Hammer characterisation

If the acceleration on the hammer head can be measured, it can be related to the contact force as,

$$a'_H = A_H f_c \tag{1}$$

where, a'_H is the acceleration on the hammer head measured upon impact, f_c is the contact force upon impact and A_H is the transfer accelerance FRF between the impact tip and hammer head. The transfer accelerance A_H characterises the hammer dynamically and acts as a calibration term to derive the force from acceleration signal.

To measure A_H, a direct and indirect calibration method can be used. In the direct method, the instrumented hammer can be hit on a calibrated force transducer and the contact force and the head acceleration can be simultaneously recorded to calculate A_H. In the indirect measurement, the instrumented hammer can be hit on a rigid mass (which has a flat frequency response in the frequency range of interest) and the acceleration on the hammer head and the rigid mass can be recorded simultaneously. The contact force can be derived as mass (of rigid mass) times acceleration of the mass (in the flat response region). Subsequently, this contact force can be used with the hammer head acceleration for calculating A_H.

3. METHODOLOGY

Let us consider an instrumented tool hammer (with accelerometer installed on its head) to be used for measuring an FRF between i (excitation DOF) and j (response DOF) on a structure as shown in Figure 1. At first, using the calibration approaches mentioned above, the Hammer FRF A_H can be measured. Next the hammer can be impacted at i and the responses on hammer head ($a'_{H,i}$) and structure (a'_j) are measured simultaneously. The mobility FRF between i and j can thus be calculated as,

$$Y_{ji} = \frac{A_H}{\omega}\frac{a'_j}{a'_{H,i}} = \frac{A_H}{\omega}T_{ji} \tag{2}$$

The term T_{ji} represents the transmissibility between the response DOF j and the response measured on the hammer head upon impact at i.

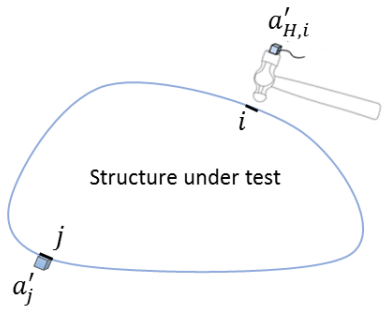

Figure 1 Schematic of FRF measurement using an instrumented tool hammer

Similarly, a mobility matrix **Y** between a multiple set of excitation DOF **i** and response DOF **j** can be measured as,

$$\mathbf{Y_{ji}} = \frac{A_H}{\omega}\mathbf{T_{ji}} \tag{3}$$

where, $\mathbf{T_{ji}}$ now represents a hammer-structure transmissibility matrix. In the current paper, a matrix is denoted by bold and uppercase letters, whereas a vector is denoted by bold and lowercase letters. Italic, non-bold letters are used to denote a single element.

For a linear time-invariant system, Equation 2 and 3 are theoretically valid for FRF measurements using the instrumented tool hammer. Further, these FRF's can in theory be also extended towards characterisation techniques which in part/fully rely on FRF measurements. As such, the application of the tool hammer will now be evaluated

for characterisation of isolators and structure borne sources which involve measurement of multiple FRF's. As a benchmark, the results from these tests will be compared with the results from an impact hammer (with force sensing).

3.1 Isolator Characterisation – Dynamic Transfer Stiffness

Consider the two configurations of the source-isolator-receiver assembly connected via single and multiple isolators as shown in Figure 2.

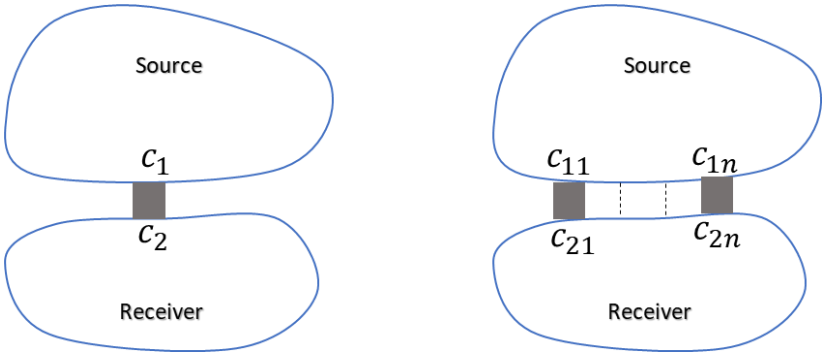

Figure 2 A source-isolator receiver assembly – single isolator case (left) and multiple isolator case (right). c_1 is the interface on the source side and c_2 is the interface on the receiver side of the isolator(s)

Concerning the single isolator case (left graphic), for isolator characterisation, the quantity of interest is the transfer dynamic stiffness which can be written in terms of impedance as,

$$K_{c_1c_2} = -\omega Z_{c_1c_2} \tag{4}$$

The transfer impedances can in turn be measured by inverting the mobility matrix measured at the interfaces (c_1 and c_2) as,

$$\begin{bmatrix} Z_{c_1c_1} & Z_{c_1c_2} \\ Z_{c_2c_1} & Z_{c_2c_2} \end{bmatrix} = \begin{bmatrix} Y_{c_1c_1} & Y_{c_1c_2} \\ Y_{c_2c_1} & Y_{c_2c_2} \end{bmatrix}^{-1} \tag{5}$$

This follows from the in-situ approach developed in [6]. For the case with multiple isolators, Equation 5 can be written as,

$$\begin{bmatrix} \mathbf{Z_{c_1c_1}} & \mathbf{Z_{c_1c_2}} \\ \mathbf{Z_{c_2c_1}} & \mathbf{Z_{c_2c_2}} \end{bmatrix} = \begin{bmatrix} \mathbf{Y_{c_1c_1}} & \mathbf{Y_{c_1c_2}} \\ \mathbf{Y_{c_2c_1}} & \mathbf{Y_{c_2c_2}} \end{bmatrix}^{-1} \tag{6}$$

where, each element of the mobility matrix is now a block matrix measured at the respective interfaces. This is an added advantage of the in-situ approach that multiple isolators can be characterised in an assembly without decoupling any substructures. For the case of the instrumented tool hammer, the same mobility matrix can be measured as,

$$\begin{bmatrix} \mathbf{Y_{c_1c_1}} & \mathbf{Y_{c_1c_2}} \\ \mathbf{Y_{c_2c_1}} & \mathbf{Y_{c_2c_2}} \end{bmatrix} = \frac{A_H}{\omega} \begin{bmatrix} \mathbf{T_{c_1c_1}} & \mathbf{T_{c_1c_2}} \\ \mathbf{T_{c_2c_1}} & \mathbf{T_{c_2c_2}} \end{bmatrix} \tag{7}$$

where, $\mathbf{T_{c_1c_1}}$ is the hammer-structure transmissibility matrix with elements of transmissibility functions measured between hammer head and response DOF at $\mathbf{c_1}$ for impact at $\mathbf{c_1}$. Similar definitions apply for $\mathbf{T_{c_2c_2}}$ and $\mathbf{T_{c_1c_2}}$.

3.2 Characterising Sources – Blocked Forces

An active structure borne source can be characterised in terms of its free velocity or blocked forces measured at the interface. The latter can be measured in-situ without the need for decoupling any substructures [7]. For a source-isolator-receiver assembly, the blocked forces of the source can be measured in-situ [7] at interface $\mathbf{c_2}$ as,

$$\mathbf{f_{bl,c_2}} = \mathbf{A^{-1}_{c_2c_2}}\mathbf{a'_{c_2}} \tag{8}$$

where, $\mathbf{f_{bl,c_2}}$ is the vector of blocked forces, $\mathbf{A_{c_2c_2}}$ is the accelerance matrix, and $\mathbf{a'_{c_2}}$ is a vector containing operational accelerations all measured at $\mathbf{c_2}$ DOF. Note that for blocked forces at $\mathbf{c_2}$, the source contains the isolators as well. With the instrumented tool hammer, the same blocked forces can be measured as,

$$\mathbf{f_{bl,c_2}} = A_H\mathbf{T^{-1}_{c_2c_2}}\mathbf{a'_{c_2}} \tag{9}$$

To validate the determined blocked forces, an on-board validation can be performed whereby the response of a remote DOF $\mathbf{k}$ on the receiver can be predicted as,

$$\mathbf{a'_k} = \mathbf{A_{kc_2}}\mathbf{f_{blc_2}} \tag{10}$$

and with the instrumented tool hammer as,

$$\mathbf{a'_k} = A_H\mathbf{T_{kc_2}}\mathbf{f_{blc_2}} \tag{11}$$

The predicted responses can be compared with the measured responses at the remote DOF to evaluate the accuracy of validation.

4. CASE STUDY

To test the validity of Equation 6 & 7, a Beam-Isolator-Plate (BIP) assembly was chosen as shown in Figure 3.

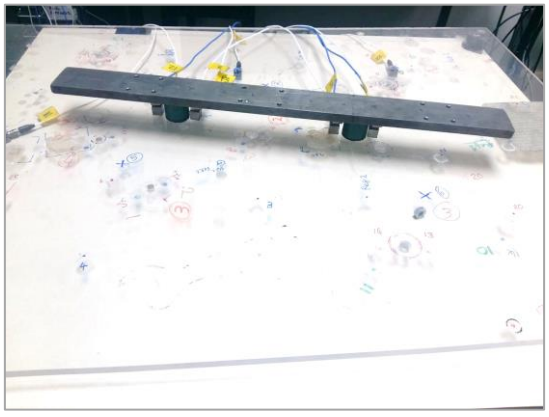

Figure 3 Beam Isolator Plate (BIP) assembly used in characterisation of dynamic stiffness of isolators

The BIP assembly provides a realistic test case where FRF's can be measured using the instrumented tool hammer. Additionally, in this assembly, the isolators can be characterised, and blocked forces can be measured to further test its application beyond standard FRF measurements. A steel beam was used as a source substructure and a Perspex plate was used as the receiver substructure connected by two cylindrical rubber isolators.

4.1 Isolator Characterisation – Remote Measurement Approach

Realistically, it would be rare to have access to DOF at both interfaces $\mathbf{c_1}$ and $\mathbf{c_2}$ for FRF measurements. Therefore, a remote measurement approach is desirable. From [6], it has been shown that the mobility matrix from Equation 6 can be remotely measured as,

$$\begin{bmatrix} \mathbf{Y_{c_1c_1}} & \mathbf{Y_{c_1c_2}} \\ \mathbf{Y_{c_2c_1}} & \mathbf{Y_{c_2c_2}} \end{bmatrix} = \begin{bmatrix} \mathbf{Y_{c_1b}} & \mathbf{0} \\ \mathbf{0} & \mathbf{Y_{c_2a}} \end{bmatrix} \begin{bmatrix} \mathbf{Y_{ba}^T} & \mathbf{0} \\ \mathbf{0} & \mathbf{Y_{ba}} \end{bmatrix}^{-1} \begin{bmatrix} \mathbf{Y_{c_1a}^T} & \mathbf{Y_{c_2a}^T} \\ \mathbf{Y_{c_1b}^T} & \mathbf{Y_{c_2b}^T} \end{bmatrix} \tag{11}$$

where, **a** are the excitation DOF on the source substructure, **b** are excitation and response DOF on the receiver (see Figure 4). The interfaces $\mathbf{c_1}$ and $\mathbf{c_2}$ are used as response DOF and no hammer excitations are required there thereby highlighting the advantage of the remote characterisation approach. Additionally, the solution can be overdetermined by choosing multiple DOF **a** and **b** on the source and receiver substructure respectively.

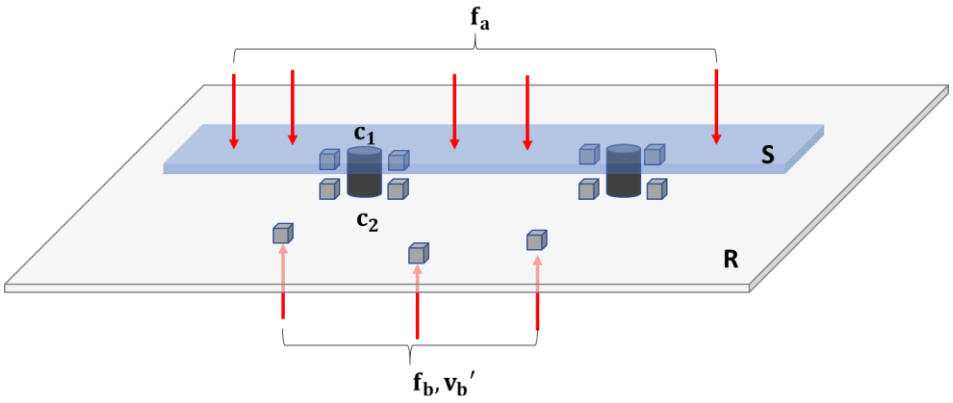

Figure 4 Schematic of remote measurements undertaken to measure dynamic stiffness (red arrows denote forces, S-source substructure, R-receiver substructure)

Following Equation 11, five **a** DOF and three **b** DOF were used. The interfaces were instrumented with a pair of closely spaced accelerometer pairs as shown in Figure 4. These responses were used to obtain an averaged response at the centre of the respective interface. Firstly, using a B&K 8206 force hammer, the mobility measurements were performed. Next, a Ball Peen hammer was instrumented with an accelerometer on the head as shown in Figure 5. For calibration, the hammer was carefully hit on the B&K force hammer tip and the force and acceleration were recorded simultaneously to give the Hammer FRF A_H. This constitutes the direct calibration approach.

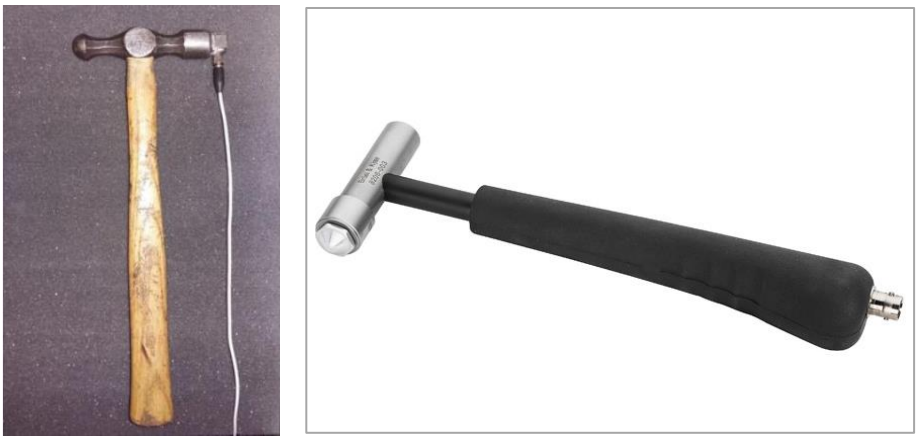

Figure 5 Instrumented tool hammer (left) and a B&K force hammer (right) used in tests

Next, using the instrumented tool hammer, the hammer-structure transmissibility matrices corresponding to Equation 11 were measured. Following Equation 3, these were converted to the corresponding mobility matrices.

4.2 Results – Dynamic Stiffness

Figure 6 shows a comparison of sample FRF's measured using the B&K force hammer and instrumented tool hammer.

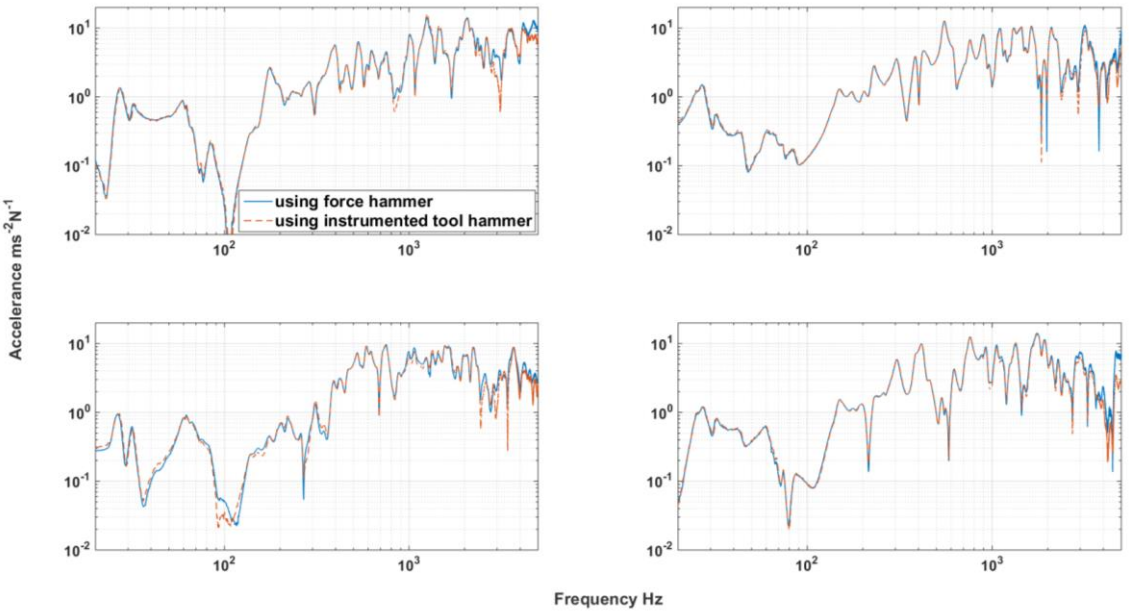

Figure 6 Sample FRF's measured on the BIP assembly using the B&K force hammer and instrumented tool hammer in 20-5000 Hz

Figure 6 shows excellent agreement between FRF measurements conducted using the B&K force hammer and instrumented tool hammer. Next, following the remote approach, the required mobility FRF's and block matrices were measured using both hammers. The ensuing mobility matrix was inverted and the relevant elements giving the transfer dynamic stiffness of isolators '1' and '2' were extracted from the impedance matrix. The results are shown in below.

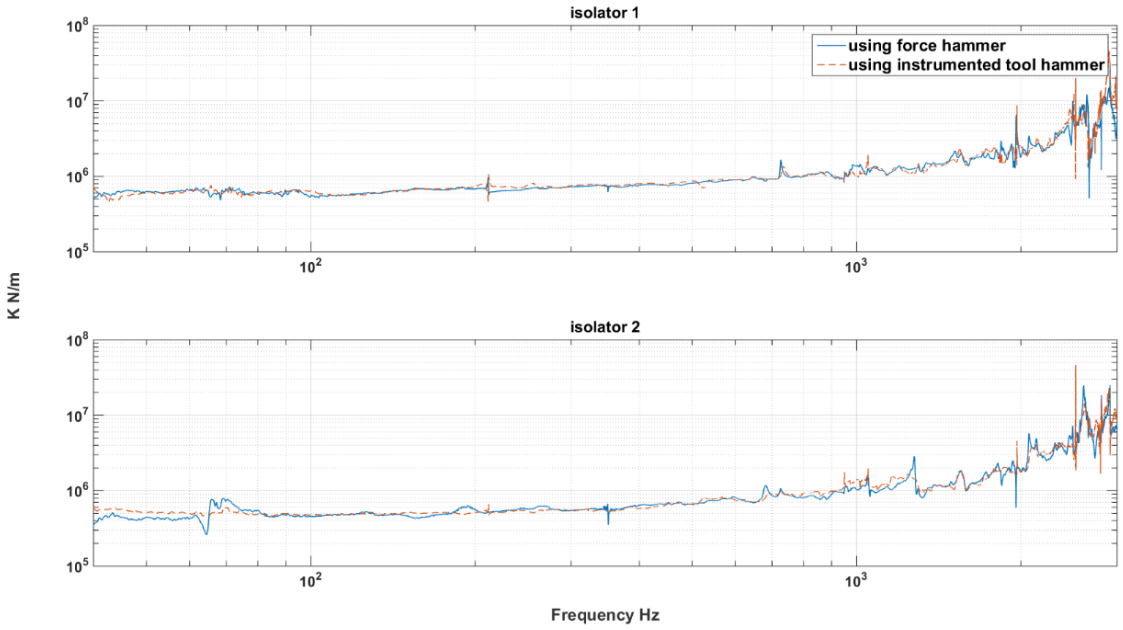

Figure 7 Comparison of dynamic stiffness of isolators from BIP assembly measured according to remote approach in 40-3000 Hz range

Figure 7 shows good agreement between the dynamic transfer stiffness measured with force hammer and instrumented tool hammer. It can be seen that the dynamic stiffness increases with frequency. Above 2.5 kHz, there are a few peaks in the dynamic stiffness curve which are artefacts arising from the resonant behaviour of source and receiver substructure.

4.3 Blocked Force Measurements and On-board Validation

The BIP assembly was also used to measure and validate blocked force characterisation using both hammer techniques. In this case, as the source beam does not have an internal driver, an artificial excitation produced by simultaneous hammer hits was applied at a remote location on the source beam to simulate an active source. The operational responses were referenced to the hammer voltage to ensure they are phase matched. Using Equation 8 and 9, the blocked forces at $\mathbf{c_2}$ were measured and are plotted in Figure 8.

Figure 8 shows that the blocked forces measured using instrumented tool hammer are in good agreement with the blocked forces measured using B&K force hammer. At low frequencies (<100 Hz), the agreement is not very well. One possible reason for this is that the tool hammer has a metal tip and is therefore not very accurate for measurements at very low frequencies. To avoid this error, it would be better to have a tool hammer with a plastic tip or an interchangeable soft tip for low frequency measurements. Nevertheless, the comparison of blocked forces alone is not a full indicator of the accuracy of characterisation measurements. An on-board validation exercise is better suited to validate the blocked forces measured in-situ [8]. In the current study, the accelerations at remote DOF **b** (see Figure 4) were predicted and compared with the measured acceleration for artificial excitations. It is important to note that in the blocked force calculations, the remote DOF **b** were not included. Therefore, results from on-board validation at **b** can be considered as a valid indicator for the accuracy of the measured blocked forces.

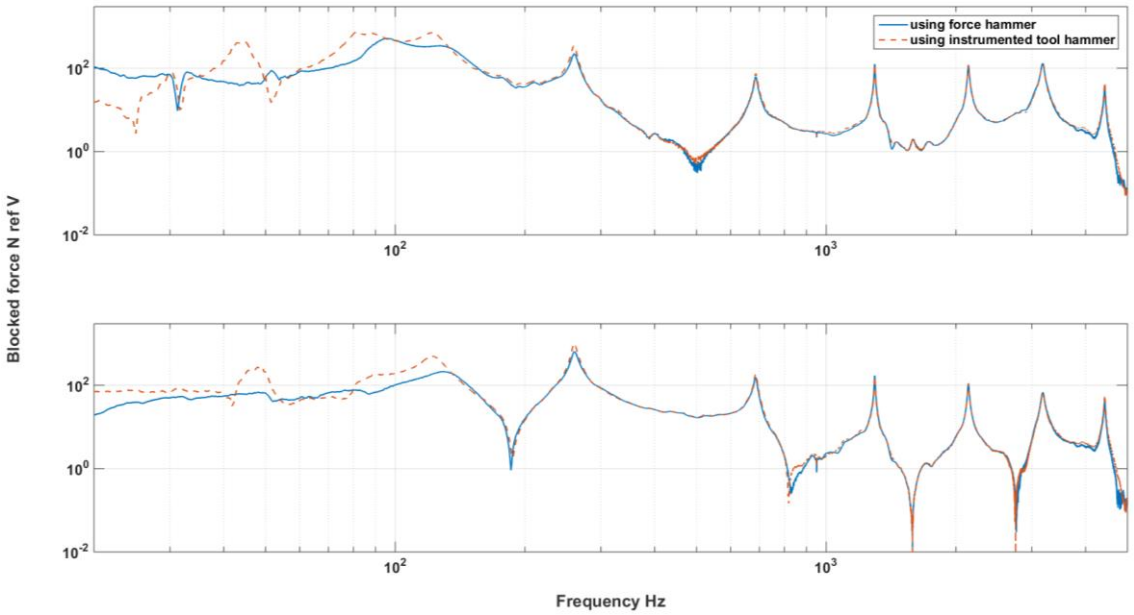

Figure 8 Comparison of blocked forces for artificial excitation measured at interface $\mathbf{c_2}$ *on BIP assembly in 20-5000 Hz range*

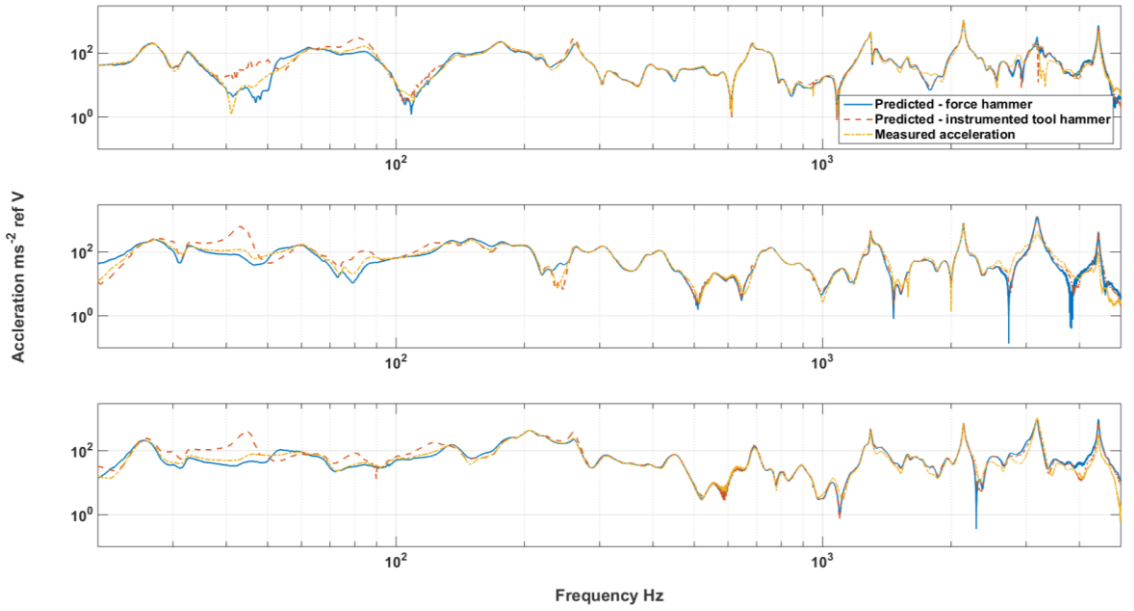

Figure 9 Onboard validation using measured blocked forces on remote receiver DOF **b** *of BIP assembly in 20-5000 Hz range*

The results from Figure 9 show that the predicted accelerations using B&K force hammer and the instrumented tool hammer are in good agreement with the measured accelerations. At low frequencies (<100 Hz), the prediction made using instrumented tool hammer is not very well. Again, the possible explanation for this is the use of a metal tip which does not offer significant low frequency impulse. Overall, this prediction exercise highlights the application and validity of the instrumented tool hammer for source characterisation and response prediction.

5. CONCLUSIONS

A novel and alternative impact testing technique is demonstrated using a tool hammer (without any inbuilt force sensor). For the application it is necessary to instrument the tool hammer with an accelerometer on the head. The first step is to dynamically characterise the hammer by 'Hammer FRF' property. Two different calibration approaches are outlined to measure the Hammer FRF. Using the instrumented tool hammer, the force referenced FRF's can be measured by measuring the hammer-structure transmissibilities and combining them with the Hammer FRF.

An instrumented tool hammer was used to evaluate the application for FRF measurement and source and isolator characterisation. A Beam-Isolator-Plate (BIP) assembly was used as a source-isolator-receiver setup for the measurements. FRF measurements were made using a B&K force hammer and the instrumented tool hammer. The former was used as a benchmark for comparison. The FRF measurements were further used in characterising the isolators in-situ. The dynamic transfer stiffness of isolators was measured remotely, and the comparison shows that the results from the instrumented tool hammer are in good agreement. Using an artificial excitation on the source beam, a structure borne source was simulated and characterised in-situ. The blocked forces obtained via standard force and instrumented tool hammer show good agreement, Additionally, an on-board validation was performed to test the validity of the measured blocked forces. The results show good agreement of the predicted response (using both hammers) and the measured responses. At low frequencies (<100 Hz), the prediction made using the tool hammer does not align very well. The possible explanation lies in the metal tip of the tool hammer which is not efficient to induce a low frequency impulse into the test structure as compared to the plastic tip of the force hammer. Overall, the studies demonstrate and validate the potential of using an instrumented tool hammer in impact testing and characterisation tests.

6. REFERENCES

1. Ole Døssing. "*Structural testing"*. Brüel & Kjær, 1987.
2. Elliott, A. S., Moorhouse, A. T., and Pavić, G. *"Moment excitation and the measurement of moment mobilities".* Journal of sound and vibration, 331, no. 11 (2012): 2499-2519.
3. Patil, N. *In-situ measurement methods for characterisation and diagnosis of airborne sound transmission through multi-layered building partitions*. PhD Thesis, University of Salford, UK (2018).
4. Lage, Y. E., Neves, M. M., Maia, N. M. M., and Tcherniak D. *"Force transmissibility versus displacement transmissibility".* Journal of Sound and Vibration, 333, no. 22 (2014): 5708-5722.
5. Howard, Carl. *"An inexpensive DIY impact hammer for vibration analysis of buildings".* Acoustics Australia 33, no. 1 (2005): 13-18.
6. Meggitt J. W., Elliott A. S., Moorhouse A. T., Lai HK. *"In situ determination of dynamic stiffness for resilient elements"*. Proceedings of the Institution of Mechanical Engineers, Part C: Journal of Mechanical Engineering Science. 230(6) (2016): 986-93.
7. Moorhouse, A. T., A. S. Elliott, and T. A. Evans. *"In situ measurement of the blocked force of structure-borne sound sources."* Journal of Sound and Vibration 325, no. 4-5 (2009): 679-685.
8. Elliott, A.S., Meggitt J.W., and Moorhouse A.T. *"Blocked forces for the characterisation of structure borne noise."* INTER-NOISE and NOISE-CON Congress and Conference Proceedings. Vol. 250. No. 1. Institute of Noise Control Engineering, (2015).